MASTER EN CAMBIO GLOBAL (CSIC-UIMP)
PROGRAMA DOCTORAL EN CAMBIO GLOBAL (CSIC-UIMP)

MEMORIA DEL PROYECTO DE INVESTIGACIÓN

Título: "*Penetration of Ultraviolet Radiation, and the spectral absorption coefficients of phytoplankton in the Eastern Pacific Ocean (Humboldt Current System)*"

Autor: Antonio Canepa Oneto
Tutor: Susana Agustí

TITULO DE PROYECTO ASOCIADO:
Campaña Oceanográfica "Humboldt 2009", Laboratorio Internacional de Cambio Global, LINCGlobal, PUC-CSIC. 2009

Tribunal: Iris Hendriks, Carlos Duarte, Romu Romero.

ABSTRACT

In the lasts decades the releases of CFC's compounds have lead a depletion rate of the ozone layer and no sign of recovery have been shown. Global change will let an increase of the pressure of Ultraviolet radiation over the marine biota, especially into the southern ocean were UVR is greater. In order to characterize the ultraviolet radiation penetration into the waters of the Humboldt Current System and to evaluate light absorption properties including the absorption in UVR wavelength of phytoplankton, five stations were performed along the coast of Chile. Results showed that the diffuse attenuation coefficients (K_d) ranged from 0,081 to 0,228 for UV-A, from 0,264 to 0,473 for UV-B and from 0,079 to 0,135 for PAR. A general latitudinal trend related with higher penetration of UVR (and PAR) into the water of the HCS in the northern part and lower in the southern part can be established. Measurements of the seston light absorption properties, suggested a major contribution of phytoplankton light absorption to the total light absorption and only northern station presented photoprotection pigments (MAA's). In terms of Global Change, the diminishing of the ozone layer will lead important consequences for the plankton community in the HCS which might have consequences in the global balance of CO_2 into the atmosphere.

INTRODUCTION

Solar ultraviolet radiation (UVR) spectrum is about 10% of the incoming energy reaching the Earth's surface, and it includes the UV-A (320-400 nm) and UV-B (280-320 nm) wavebands (Helbling and Zagarese, 2003). The intensity at which UVR reach the surface, isn't constant for the entire planet depending of the thickness of the ozone layer. The general trend is higher levels near the equator and lower levels near the poles (Heberlein and Bournay, 2009; Jarah *et al.*, 2009). In the lasts decades the release of CFC's compounds have lead a depletion rate of the ozone layer near to 4 DU $year^{-1}$ between 1979 and 1995 and there are few or non sign of recovery (Weatherhead and Andersen, 2006). The failure in recovery of the ozone layer isn't fully understood but seems to be related with the emissions of other chemicals like nitrous oxide (N_2O) used as fertilizers (Weatherhead and Andersen, 2006; Ravishankara *et al.*, 2009). The maximum lost of ozone is reached every year during the austral spring over the Antarctica, resulting in the so called "ozone hole" which represent a lost about 50% of total ozone measured in the area (Smith *et al.*, 1992). Due to the nonlinearity of the effects of some components of the global change over the climate and other general regulation process of the earth system (Duarte *et al.*, 2009), an increase of the pressure of UVR over the biota (mostly marine biota at surface) is expected (Häder *et al.*, 1995; Helbling and Zagarese, 2003; Häder *et al.*, 2007; Llabrés *et al.*, *Submitted*). Due to this negligible recovery of the Ozone layer (Hardy and Gucinski, 1989; Smith *et al.*, 1992; Solomon, 1999), the amount of UVR (mostly UV-B) that reaches the earth, is expected to keep increasing as the damage for terrestrial and aquatic organism. UVR damage into aquatic ecosystems correlates strongly with the penetration of UV radiation into the water column, and UV-B has a stronger deleterious effect than UV-A. Exposure to solar UVR can reduce productivity, affect reproduction and development, and increase the mutation rate in phytoplankton, macro-algae, eggs, and larval stages of fish and other aquatic animals (Hardy and Gucinski, 1989; Häder et al., 2007; Llabrés et al., *Submitted*). For autotrophic community the most important effects are the damages over DNA, bleach pigments, increases membrane permeability and depresses nitrate and

phosphorus uptake. The ultimate impacts are reduction in primary production, changes in species composition and subsequent influence on the food web (Yaping *et al.*, 2010). Generally, phytoplankton has two mechanisms to face the UVR damage. By one hand they can tolerate the irradiation of UVR showing differential growing rates at different depths, and by the other hand, phytoplankton can resist damage from UVR developing various screening mechanisms both physical (mucus, sporopollenin, multiple cell walls) and chemical like some mycosporine-like amino acids (MAA's). These compounds are characterized by a cyclohexenone or cyclohexenimine chromophore conjugated with the nitrogen substituent of an amino acid and have UV-absorption maxima in the range 310–360 nm (Dunlap and Shick, 1998), have been identified in a wide phyletic assortment of marine organisms and may provide partial photoprotection from ultraviolet (UV) radiation (Whitehead and Vernet, 2000; Singh *et al.*, 2008).

The amount of solar radiation, including UVR, which penetrates into the water column, not only depends on the amount of radiation reaching the ocean surface but also on the inherent and apparent optical properties of the sea. Inherent optical properties (IOP) depends on the absorption and scattering properties of the water itself and its constituents (particles and dissolved substances), whereas apparent optical properties (AOP), depend both on IOP and on the underwater light field in which they are measured (Booth and Morrow, 1997; Helbling and Zagarese, 2003; Tedetti and Sempéré, 2006). Penetration of UVR into natural waters can be empirically described by two measurements that are wave-length dependent and interrelated: the downwelling diffuse attenuation coefficient (K_d) and the percent attenuation depth ($Z_{n\%}$) (Helbling and Zagarese, 2003). Diffuse attenuation coefficient (K_d) is the most widely measured AOP, and is basically dependent on the attenuation of light in water, influenced by the angle of incident light and the absorption and backscattering of underwater (Helbling and Zagarese, 2003). Percent attenuation depth ($Z_{n\%}$), measures the depth at witch irradiance (wavelength-dependant) is reduced from 100%, into superficial waters to a **n**% (in a uniformly mixed water column). Calculations of $Z_{1\%}$ and $Z_{10\%}$ have been used increasingly in the UV literature (Häder *et al.*, 1998; Helbling and Zagarese, 2003) but infer significance primarily from the PAR waveband where $Z_{1\%}$ is considered the bottom and $Z_{10\%}$ the midpoint of the euphotic zone for photosynthesis (Helbling and Zagarese, 2003).

UVR levels that reach the surface over the southern hemisphere are greater than those received into the northern hemisphere and particularly the effect of the ozone hole could have important consequences over the biota of the southern ocean (Atkinson, 1997). Few measurements of UVR penetration in natural waters have been made on the South Pacific Ocean, with the world clearest waters to UV found in the anticyclonic South Pacific Gyre (Tedetti and Sempéré, 2006; Tedetti *et al.*, 2007). This water represents a particular ecosystem characterized as "hyper-oligotrophic" due to the low amounts of nutrients (*op. cit.*). By the other hand, in the south east pacific occurs a major system of currents, the Humboldt Current System (HCS), which remains one of the less studies ecosystems. The HCS includes the upwelling ecosystems off Peru and Chile, and is one of the most productive marine systems in the world (Morales and Lange, 2004). In Chile the upwelling areas can be separated in a northern continous-upwelling area (18-30 °S) and a central-south strongly seasonal upwelling area (30 – 40° S) both contributing to a high biological, economical, and socio-cultural fishery zone (Thiel *et al.*, 2007). One feature of he HCS is its latitudinal range, showing conspicuous gradients of temperature, salinity and oxygen concentration, among others (Fernández and Brante, 2003; Fariña *et al.*, 2008; Fernández *et al.*, 2009). Those gradients have important consequences into the biology of the organisms that lives in

those waters showing strong gradients into the developmental modes, breeding effort, and latitudinal range distribution (Fernández *et al.*, 2000; Broitman *et al.*, 2001; Fernández *et al.*, 2009). From all these environmental stressor one of the less studied is the ultraviolet radiation (UVR), which its effects has been recently assessed only in the intertidal zone (Véliz *et al.*, 2006; Andrés *et al.*, 2007) and in coastal embayment waters, showing important effects for the communities studied (Wahl *et al.*, 2004).

The objectives of this study are to characterize the ultraviolet radiation penetration into the waters of the Humboldt Current System, located in the South Pacific and able to be impacted by the higher increase in UVR at this area of the earth. Also to evaluate light absorption properties including the absorption in UVR wavelength of phytoplankton and discuss some possible consequences for the phytoplankton community.

MATERIALS AND METHODS

Humboldt 2009 Campaign

Data were taken during the Humboldt-2009 cruise on board R/V Hesperides. The cruise started in the Patagonian channels (54.80º S) on March 5 and followed the HCS north, until the proximity of Antofagasta, Chile on march 15 (23.85 º S). On this track five stations were conducted to i) perform underwater profiles of ultraviolet radiation penetration and ii) collect surface water samples to evaluate the spectral absorption of phytoplankton, covering a latitudinal gradient (Fig 1).

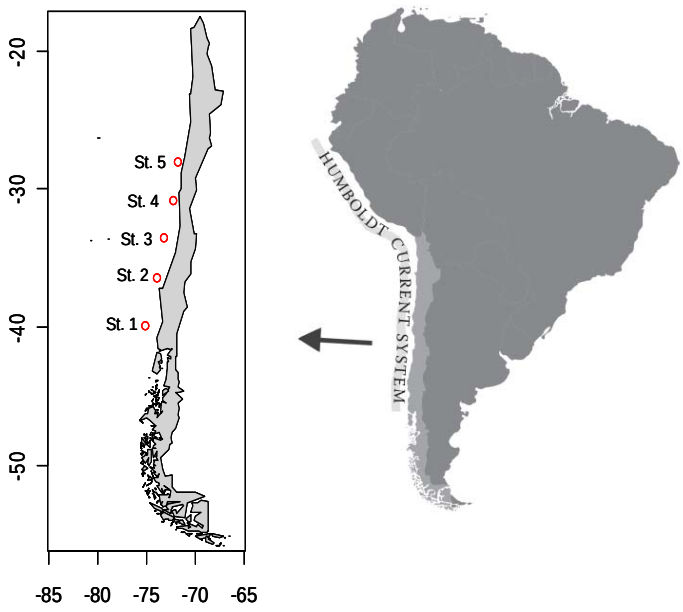

Figure 1. Latitudinal orientation of the five stations were UVR penetration profiles were done, following the Humboldt Current System (Modified from (Thiel *et al.*, 2007)).

Incident solar and ultraviolet radiations were obtained continuously, for all campaign, from a meteorological station (Weatherlink Vantage Pro Davis Co) located on board the R/V Hespérides. Photosynthetic Active Radiation (PAR) was measured with a solar radiation 6450 Davis sensor (from 400-1100 nm) every 5 minutes. Data of UV was provided as "UV" Index.

Underwater Ultraviolet Radiation (UVR) and Photosynthetically Active Radiation (PAR) profiles were performed on five (5) stations around noon by using a profiler PUV-2500 radiometer (Biospherical Instruments) which measures UVR at 6 wavelengths: 305, 313, 320, 340, 380, 395 nm, with 10 nm Full-Width Half-Maximum (FWHM) standard, except 305 (controlled by atmospheric ozone cut off). The instrument also has a PAR (400-700 nm) sensor. Data of different wavelengths were integrated into broad range of ultraviolet A "UV-A" (320-395nm) and ultraviolet B "UV-B" (305-313 nm) radiation (Pelletier *et al.*, 2006) and data of incident UVR for those stations is presented as daily maximum "UV index".

Data Analysis

For all the analyses and graphs the "R" language and environment for statistical computing and graphics was used (R Development Core Team, 2010).

The diffuse attenuation coefficient (K_d) were obtained from the slope of linear regressions of natural logarithmic down welling irradiance against depth.

The amount of UVR (and PAR) at different depths and stations were determined using the Beer-Lambert's equation:

$$\mathbf{I}_{(z,\lambda)} = \mathbf{I}_{(0,\lambda)} \mathbf{x}\ \mathbf{EXP}^{(-\mathbf{Kd}\ \mathbf{x}\ \mathbf{Z})}$$

Were $I_{(z,\lambda)}$ is the irradiance at depth (Z), for each wavelength range (UV-A, UV-B and PAR); $I_{(0,\lambda)}$ is the irradiance recorded at surface* (z = 0), for each wavelength range (UV-A, UV-B and PAR); Kd is the diffusion attenuation coefficient (explained above) and Z is the depth by which irradiance was measured.

* The Irradiance at surface was calculated, for each station, as the average of incidental irradiance in the first 30 centimetres.

Percent attenuation depth ($Z_{n\%}$, m^{-1}) was calculated using:

$$\mathbf{Z}_{(n\%,\ \lambda)} = \mathbf{ln}_{(n\%)} / \mathbf{K_d}_{(\lambda)},$$

Where $_{n\%}$ is the irradiance percentage of its surface value; and the K_d is The diffuse attenuation coefficient (Tedetti *et al.*, 2007).

Comparisons of ultraviolet radiation penetration among different Stations were performed using ANCOVA (Quinn and Keough, 2002). Due the profiles has unequal number of observations of depth among stations, the resulting data sets has different interval sampling rate. ANCOVA test is sensible to this difference (Crawley, 2007), and to solve this, the diffusion attenuation coefficient (K_d) was used to construct equal interval sampling rate of profiles from different stations. For visual inspection of the ultraviolet penetration over the four stations Three-Dimensional Plots contour plots were done using "akima" package of R software (Gebhardt *et al.*, 2009).

Light Absorption by Phytoplankton

The light absorption properties of seston were measured on seawater particles concentrated on filters (Agustí and Cruzado, 1992; Lieselotte and Dale, 1997; Varela *et al.*, 1998). Seawater particles were collected from the surface (5 meters) waters at the stations where UVR profiles were taken. The seston samples where obtained after filter a variable volume of water with Whatman GF/F filters. Filters were kept wet on petri disks with Milli-Q water and conserved refrigerated in the dark until spectrophotometric measurements. The optical density of the filters (OD_f) was measured in a spectrophotometer (Shimadzu) using a clean-water saturated Whatman GF/F filter as a blank (Agustí and Cruzado, 1992). OD_f was measured at several wavelengths covering the UV-A, B and PAR spectra. Absorption coefficient (**a**) was calculated using:

$$\mathbf{a}_{(\lambda)} = \mathbf{2{,}3\ OD_{f\,(\lambda)}\ C\ /\ V\ \beta_{(\lambda)}}$$

Where λ = wavelength (nm); 2.3 is the factor to convert base 10 logarithms to natural logarithms; C = clearance area of the filter (m^2); V = volume of seawater filtered (m^3); and β = wavelength-dependent pathlength amplification factor of the filters, following (Bricaud and Stramski, 1990).

$$\beta_{(\lambda)} = \mathbf{1{,}63\ OD_{f\,(\lambda)}^{-0{,}22}}$$

The absorption coefficient for total Particles ($\mathbf{a_p}$) was corrected by subtracting the absorption at 750 nm (Varela et al., 1998) for all wavelength range. To obtain the absorption coefficient of non algal particles ($\mathbf{a_d}$), an indirect method was used (Bricaud and Stramski, 1990; Lieselotte and Dale, 1997), following:

$$\mathbf{a_{d\,(\lambda)} = A\ EXP\ (-S\ \lambda) + a_p(750) - A\ EXP\ (-750\ S)}$$

Where A and S were obtained from the following systems of equations, using a quasi-Newton estimation technique (Varela et al., 1998):

1) $0.99\ A\ EXP(-380\ S) - A\ EXP(-505\ S) = 0{,}99\ a_p(380) - a_p(505)$
2) $A\ EXP(-580\ S) - 0.92\ A\ EXP(-692.5\ S) = a_p(580) - 0{,}92\ a_p(692{,}5)$

Finally to calculate the light absorption coefficient for phytoplankton ($\mathbf{a_{ph}}$) the following relation was used:

$$\mathbf{a_{ph} = a_p - a_d}$$

RESULTS

The incident UVR showed a general pattern of increasing towards the Equator (Figure 2), and the values recorded from all campaign, ranged broadly from 1 to 11 UV index. In the five stations where the UVR penetration profiles were done, the UV index (measured as daily maximum levels) ranged from 6 to 11 (Table 1).

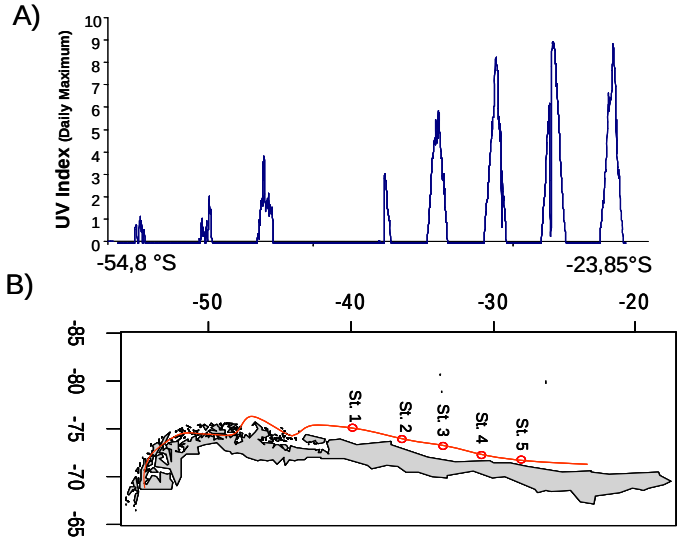

Figure 2. Latitudinal variation of the UV "Index" along the "Humboldt 2009" campaign. In the upwards graph (A) the latitudinal values of UV index are shown except for the "Golfo de Penas" area, where the meteorological station stop working due to the hard seas condition. In the lower graph (B) the latitudinal track of the Humboldt Campaign is shown, as well the position of the five stations where underwater profiles were done.

Table 1. Ultraviolet incident levels (measured as daily maximum index), diffusion coefficient (Kd), and deep of penetration for 1% and 10 % for wavelengths 305, 313 and 320 nm (UV-B), 340, 380 and 395 nm (UV-A) and PAR (A), and integrated values for whole UV-B and UV-A range (B).

A)

			UV-B									UV-A									PAR		
Station	Location	UV-Index	305 nm			313 nm			320 nm			340 nm			380 nm			395 nm			400-700 nm		
			Kd	Z (1%)	Z (10%)	Kd	Z (1%)	Z (10%)	Kd	Z (1%)	Z (10%)	Kd	Z (1%)	Z (10%)	Kd	Z (1%)	Z (10%)	Kd	Z (1%)	Z (10%)	Kd	Z (1%)	Z (10%)
1	39°S - 75°W	6	0,531	8,67	4,34	0,507	9,08	4,54	0,468	9,84	4,92	0,357	12,90	6,45	0,237	19,43	9,72	0,217	21,22	10,61	0,135	34,11	17,06
2	36°S - 74°W	8	0,409	11,26	5,63	0,353	13,05	6,52	0,327	14,08	7,04	0,247	18,64	9,32	0,169	27,25	13,62	0,155	29,71	14,86	0,111	41,49	20,74
3	33°S - 73°W	9	0,299	15,40	7,70	0,32	14,39	7,20	0,261	17,64	8,82	0,179	25,73	12,86	0,118	39,03	19,51	0,082	56,16	28,08	0,08	57,56	28,78
4	30°S - 72°W	9	0,299	15,40	7,70	0,31	14,86	7,43	0,275	16,75	8,37	0,237	19,43	9,72	0,168	27,41	13,71	0,157	29,33	14,67	0,103	44,71	22,36
5	28°S - 71°W	11	0,349	13,20	6,60	0,288	15,99	8,00	0,262	17,58	8,79	0,188	24,50	12,25	0,112	41,12	20,56	0,098	46,99	23,50	0,079	58,29	29,15

B)

Station	Location	UV-Index	Diffusion Coefficient (Kd)			UV-B Penetration (m)		UV-A Penetration (m)		PAR Penetration (m)	
			UV-B	UV-A	PAR	Z (1%)	Z (10%)	Z (1%)	Z (10%)	Z (1%)	Z (10%)
1	39°S - 75°W	6	0,473	0,228	0,135	9,7	4,9	20,2	10,1	34,1	17,1
2	36°S - 74°W	8	0,338	0,169	0,111	13,6	6,8	27,2	13,6	41,5	20,7
3	33°S - 73°W	9	0,264	0,081	0,080	17,4	8,7	56,9	28,4	57,6	28,8
4	30°S - 72°W	9	0,273	0,119	0,079	16,9	8,4	38,7	19,3	58,3	29,1
5	28°S - 71°W	11	0,294	0,155	0,103	15,6	7,8	29,7	14,9	44,7	22,4

The surface UVR received varied among station, but in all of them the general patterns was that the irradiance diminished quickly with depth in all station. UV-B shows a greater decline than UV-A (Figure 3).

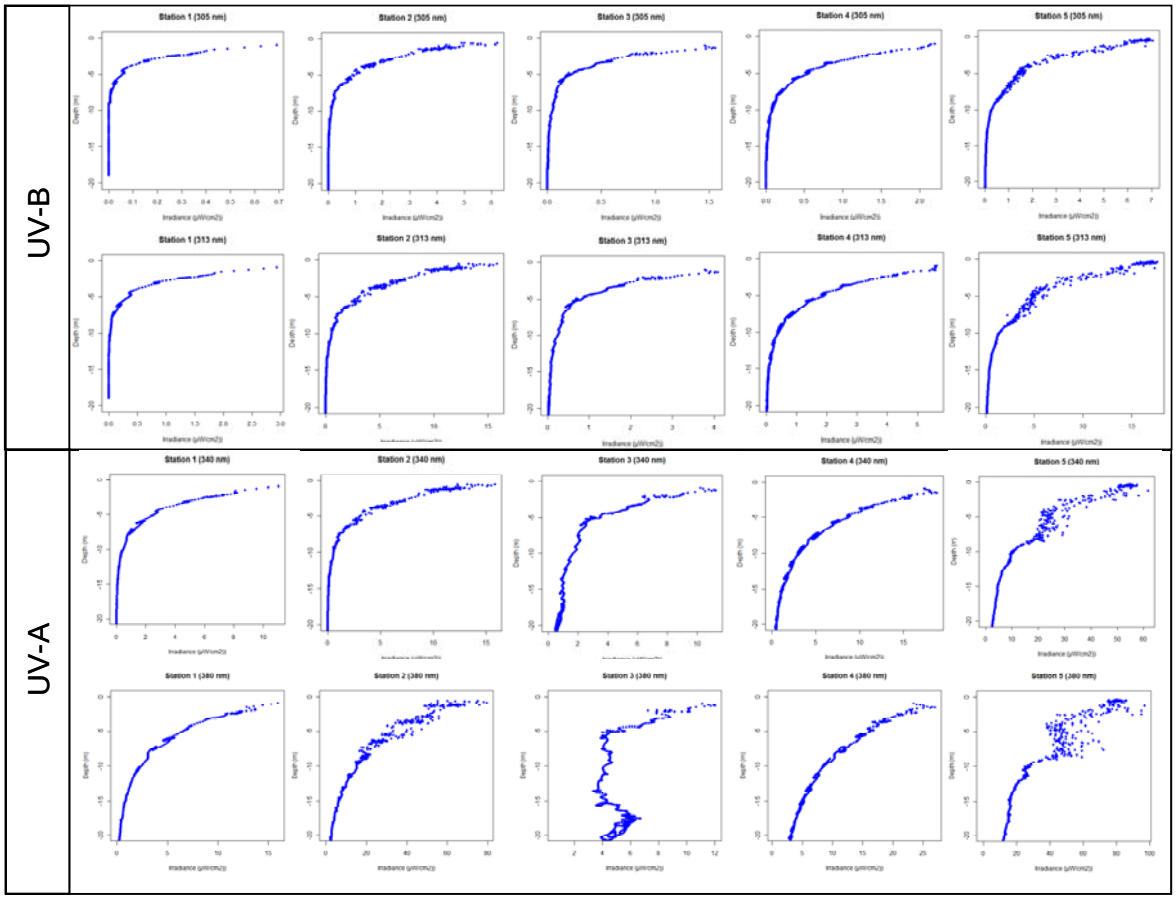

Figure 3. Irradiance downwelling attenuation of UV-B (305 and 313 nm) and UV-A (340 and 340 nm) recorded at five stations. Axes are in different scales due to the particular radiation properties recorded at each station and water penetration characteristic of each station.

From the regression of irradiance (natural logarithm of irradiance) versus depth a total of five diffuse attenuation coefficients (K_d) were obtained. The slopes for each station are shown in figure 4.

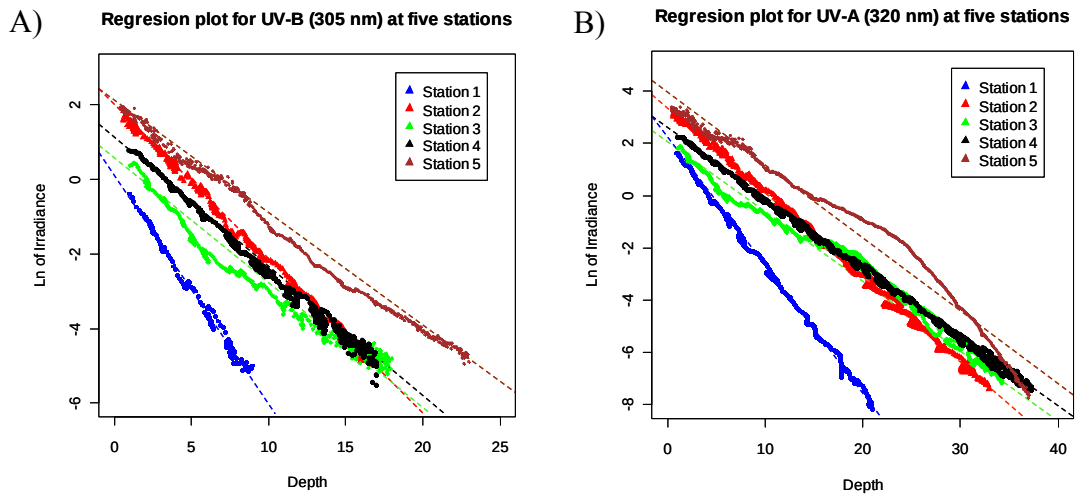

Figure 4. Regression plots showing UVR penetration against depth for UV-B (305 nm, A) and UV-A (320 nm, B) for the five stations surveyed. Dashed lines show the adjusted regression line where slopes (K_d) were obtained.

Diffuse attenuation coefficients (K_d) ranged from 0,081 to 0,228 for UV-A, from 0,264 to 0,473 for UV-B and from 0,079 to 0,135 for PAR. The maximum values were recorded at the southernmost station (N°1), coinciding with the lower transparency of the water column. Thus a general pattern of decreasing values of K_d to the Equator was observed, except for the station N° 3 were lowest values were found. The depth to which 1 % of the UV-B and UV-A surface's radiation penetrated, increased from 9,7 and 20,2 meters in the southernmost station (N°1) to 15,6 and 29,7 meters at the northernmost station (N°5), respectively (Table 1). This pattern of increased penetration of surface UVR, along the transect gradient is shown in figure 5.

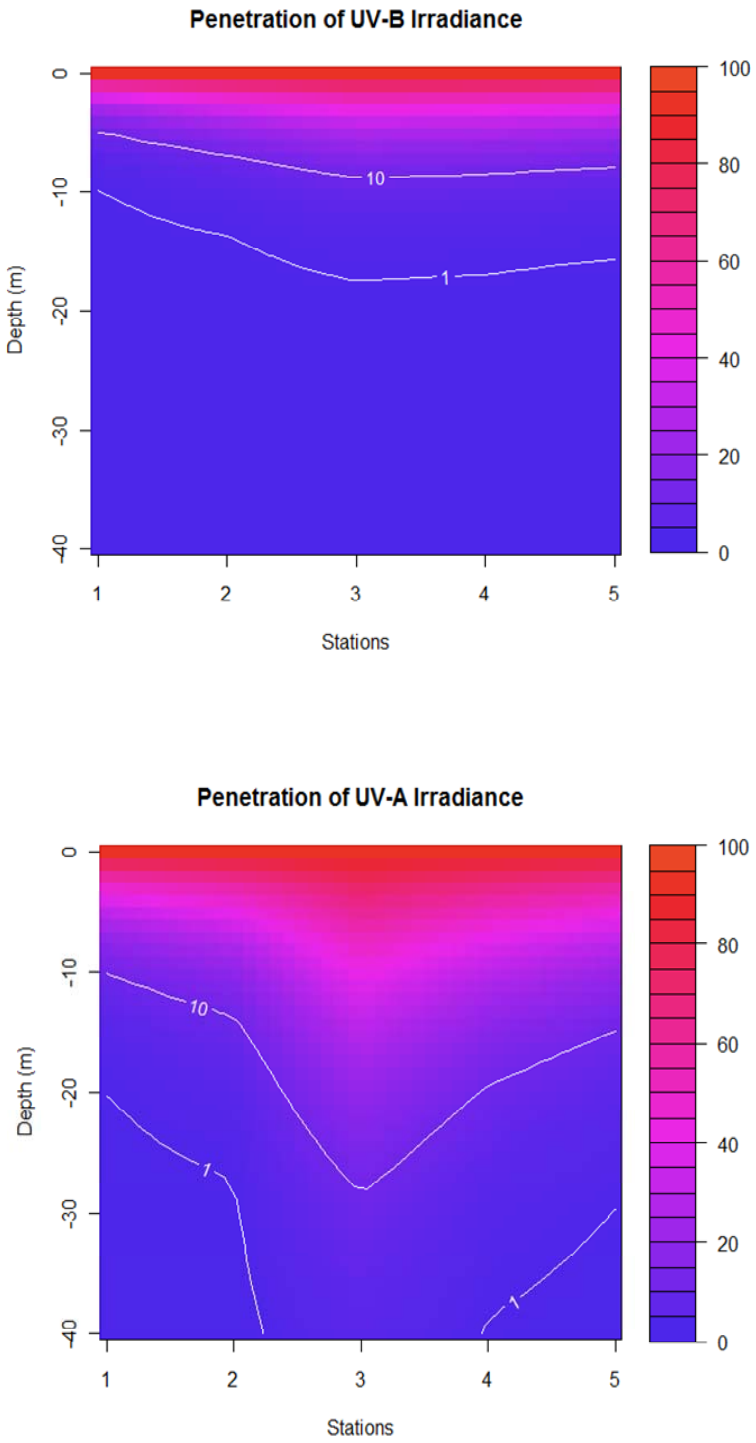

Figure 5. Three dimensions plots showing the ultraviolet irradiance penetration, measured as the surface percentage, of ultraviolet B (upper plot) and ultraviolet A (lower plot). In both cases the depth where 1% and 10% is reached is highlighted.

Results of the Analysis of Covariance (ANCOVA) showed significantly relationship among ln of irradiance with depth and station, showing a clear effect of the depth and the latitudinal gradient over the underwater penetration of the irradiance for both UV-A and UV-B (ANCOVA p< 0,001) (Table 2). Furthermore, the ANCOVA model showed significant interaction among the predictor variable (depth) and the covariate (station) showing significantly differences among slopes of the four stations for both UV-A and UV-B (Table 2).

Table 2. Summary results from the ANCOVA analysis. All the variables tested were significant and also the interaction between the explanatory variable (Depth) and the covariate (Station), for both UV-A and UV-B.

UV-A	*Df*	*Sum Sq*	*Mean Sq*	*F value*	**Pr(>F)**
Station	1	126.25	126.25	149.519	**< 2.2e-16** **
Depth	1	649.20	649.20	768.824	**< 2.2e-16** **
Station **x** Depth	1	22.05	22.05	26.114	**7.4e-15** **
Residuals	201	169.73	0.84		
UV-B	*Df*	*Sum Sq*	*Mean Sq*	*F value*	**Pr(>F)**
Station	1	519.62	519.62	337.384	**< 2.2e-16** **
Depth	1	3098.97	3098.97	2013.328	**< 2.2e-16** **
Station **x** Depth	1	101.74	101.74	66.096	**4.3e-16** **
Residuals	201	309.38	1.54		

Measurements of the seston light absorption properties, suggested a major contribution of phytoplankton light absorption to the total light absorption (Figure 6). The spectra at the different stations showed two major peaks of absorption, one into the range between 660 y 680 nm, corresponding to one of the absorption peaks of Chlorophyll a in vivo, and the higher absorption peak observed between 400-480 nm, which correspond to the major peak of light absorption by Chlorophyll a in vivo (around 440 nm).

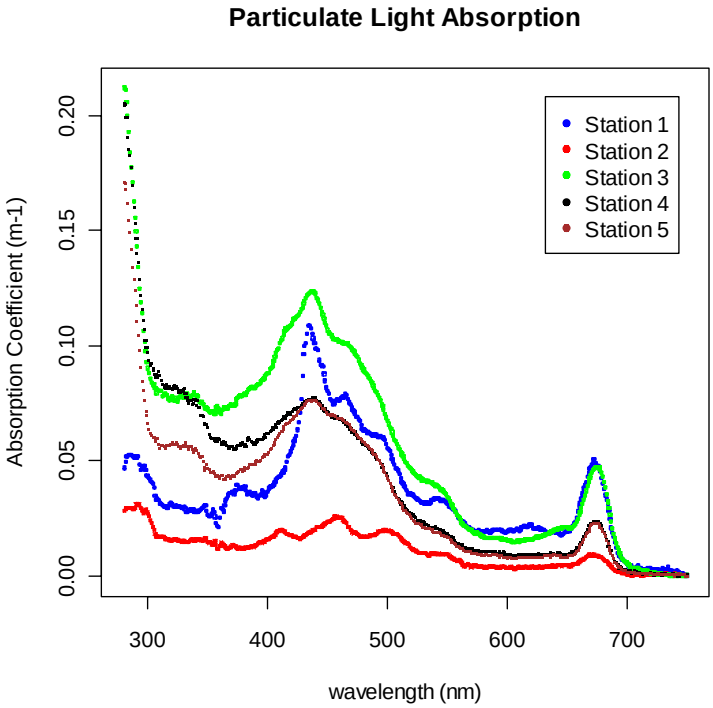

Figure 6. Spectral values of the absorption coefficient (m-1) by particulate matter at the five stations. Major absorption peaks observed in the visible bands corresponded to those of photosynthetic pigments and, for some of the stations, absorption peaks in the UV bands in the range of MAA's photoprotection pigments were also detected.

The method used to calculate the detrital (non-algal) absorption coefficient (a_d) (Bricaud and Stramski, 1990; Agustí and Cruzado, 1992) resulted in five values of A and S from the exponential equation. Results for the five stations are shown into table 3. There is a general trend of diminishing absorption of detrital matter with higher wavelengths as expected. In stations 1 and 2 the absorption of detrital matter was wrong predicted by the quasi-Newton estimation technique gave negative values, so for this stations the values of absorption coefficients due to detrital matter (a_d) were considered to be negligible, and the values of phytoplankton a_{ph} dominated those of a_p (figure 7, stations 1 and 2). For the stations 3, 4 and 5 the spectral absorption coefficients of phytoplankton a_{ph} were lower than the a_p, due to detrital absorption and the shape of the curve remains equal to that of phytoplankton absorption. At the lowest wavelengths measured (below 300 nm) the peaks in absorption observed could be originated by the filter absorption (galss fiber material) so they were not interpreted. For the station 1 and 2 no evidence of absorption peaks at the UVB range was observed; however station 3, 4 and 5 showed soft peaks at the range of 330-340 nm, indicative of the presence of UV photoprotection pigments (figure 7 y 8).

Table 3. Summary results from the solution of the of the system equations proposed by (Bricaud and Stramski, 1990).

Stations	A	S
1	-0,117134	0,00196
2	-0,107985	0,0053800
3	0,306182	0,0057000
4	0,343745	0,0058
5	0,103104	0,0038245

The depth at which the highest concentration in autotrophic biomass observed, the deep chlorophyll maximum (DCM), also varied among stations. The highest depth was achieved at northern stations (figure 9) ($R=0,77$; $p<0,001$) . Results of the linear model and significance values are shown in table 4.

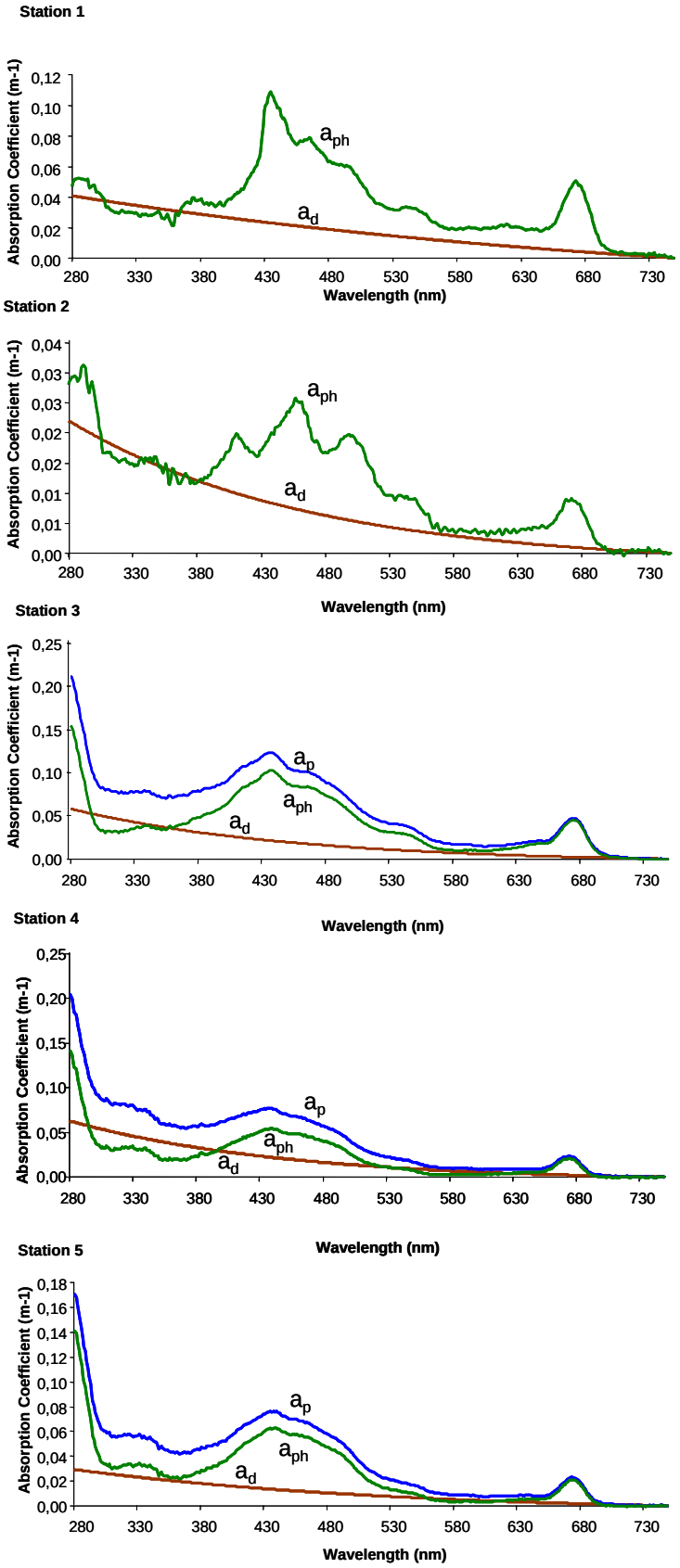

Figure 7. Decomposition of the spectral values of absorption coefficient of particulate matter (a_p) into absorption coefficient of detrital (non-algal) particles (a_d) and living phytoplankton a_{ph}, for the five stations surveyed. Station 3, 4 and 5 shows absorption peaks at 330-340 nm, indicative of the presence of photoprotection pigments.

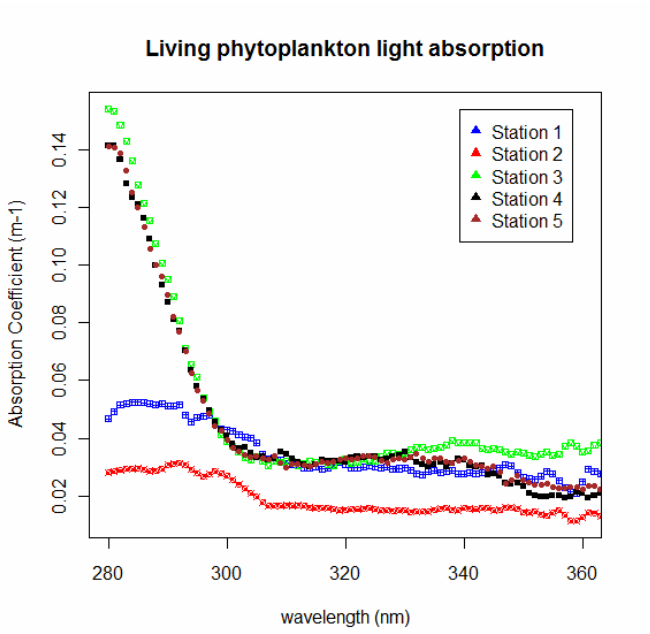

Figure 8. Plot showing the phytoplankton absorption coefficient (m-1) for the range of 280 to 360 nm.

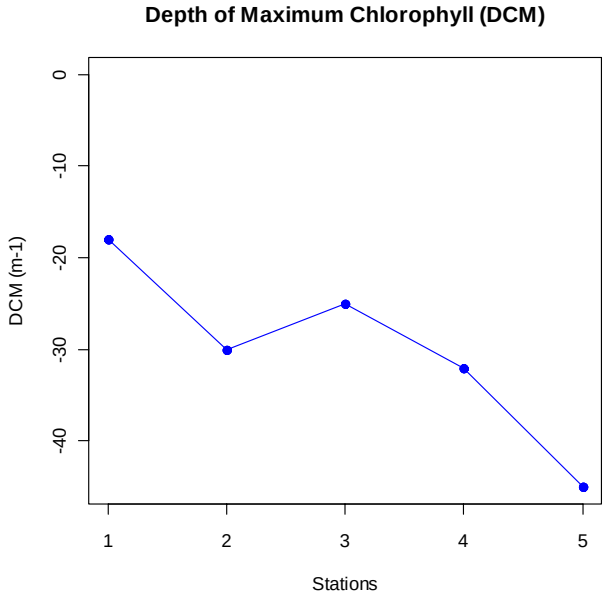

Figure 9. Deep of the maximum chlorophyll concentration among the stations. Station 1 is the southernmost station and 5 is the northernmost one.

Table 4. Summary results from the linear regression (Linear Model, (Crawley, 2007)), between the depth at which the maximum concentration of chlorophyll was found and the latitudinal range (stations).

Coefficients: adjusted R-squared: 0.77 F-statistic: 48.3, p-value: 1.007e-05				
Linear Model	Estimate	Std. Error	t value	Pr(>|t|)
(Intercept)	-13.200	2.6734	-4.939	0.000270 ***
Stations	-5.600	0.8057	-6.950	0.000001 ***

DISCUSION

The Ultraviolet Radiation (UVR) measured as UV-Index showed a clear pattern of increase with lower latitudes, so the amount of energy that reach the surface of waters is greater in the northern part than the southern part of the HCS. Those results are in agreement with those reported for continental Chile (Cabrera *et al.*, 1995). This pattern of irradiance can be explained at least for two principal factors, one is the differential cloud cover registered over the coastal margin of Chile, being the southern part normally covered with dense clouds from cyclonic front due to the west driven winds, called the Polar low pressure (Latif and Keenlyside, 2008). By the other hand in the central and northern part of Chile, the occurrence of the anticyclonic (high pressure) leads into clear sky partially uncovered with clouds over the year, representing one of the clearest skies of the earth (Power and Smith, 2007; Latif and Keenlyside, 2008). The other factor is that the total ozone layer diminishes from the equator to the poles and explains (in certain vain) the radiative balance over the earth system (Heberlein and Bournay, 2009; Jarah et al., 2009). Is important to point out, that even the latitudinal variation of UVR along the coast of Chile, the high values recorded trough Humboldt campaign (maximum UV index equals to 11), aren't expected be the maximum values of UVR reaching the ocean surface, due the date of the cruise match with the late summer (begging of Autumn) and even higher values should be recorded in the summer season (Cabrera et al., 1995).

Both UV-A and UV- B decreased irradiance with depth, showing greater depletion in the southern stations than in the northern ones. The same pattern is obtained when values of the Diffusion Attenuation Coefficient (K_d) are compared (Table 1 and figure 4). Those values are representative of water with high nutrients and levels of high dissolved organic matter, characteristic of productive waters (Booth and Morrow, 1997; Tedetti and Sempéré, 2006; Tedetti et al., 2007). In all the stations UV-A penetrate deeper than the UV-B, and station number 3 was, particularly, transparent to UV-A. Due to the significant effect of the interaction between latitude (stations) over the decrease of irradiance against depth (ANCOVA $p < 0{,}001$) (Quinn and Keough, 2002) (see Table 2), a latitudinal trend can be established. This trend is related with higher penetration of UVR (and PAR) into the water of the HCS in the northern part and lower in the southern part (figure 5). These results are in agreement with those found by Montecino and Pizarro (1995). (Montecino and Pizarro, 1995)Tedetti *et al.* (2007) found higher values of K_d at 35° S (305 nm, $k_d = 0{,}756$) but this profile was done during summer (6 December 2004), so higher productivity is expected to diminish the clarity of water and give high values of K_d, this could be certain due to at this station they recorded the higher productivity of their study and because high temporal variation have been found in the optical properties of this waters (Montecino and Pizarro, 1995; Morel *et al.*, 2007; Tedetti et al., 2007). Because of the latitudinal gradient of higher penetration of UVR into water, showed in this study, the depth at which the 1 and 10 % of UV-A and B reached was greater in the northern stations (3, 4 and 5) than in the southern stations (1 and 2). The amount of damage produced by the UVR in aquatic systems is proportional to the UVR penetration (Häder et al., 2007), so we can expect damage related to UVR and possible association with global change be more strong into the northern part of the HCS than in the south. This effect is still been studied (Godoy *et al.*, *in prep*) but the general conclusions are that the productivity of autotrophic communities into the HCS, diminished with the UVR (measured as Net Community Production) and the decrease was greater in the northern stations than in the southern stations (in all of them the effect of UV-B had the same consequences). Based in this

data and the data from Godoy *et al.* (*in prep*) we can conclude that the UVR effect over the HCS leads a more heterotrophic community and the effect for other organisms (larvae, eggs, among other) should be greater in the northern part than in the southern part. More research is needed in order to evaluate the dose-related effect of irradiance and penetration in these waters. Even that marine organism (among others) have specialized mechanism to protect from UVR, these mechanism have conflicting selection pressures (Häder et al., 2007) and with the expected effects of global change over the UVR irradiance more stress and possible more metabolic cost for these organism are expected to occur in these waters.

The light absorption by particles was dominated by the absorption of phytoplankton (figure 6 and 7). Examination of the absorption spectra by the autotrophic plankton component revealed evidence of the presence of UVB photoprotection pigments for stations 3, 4 and 5 (the northern ones) as have been found into the Southern Ocean (Smith et al., 1992). This lack of photoprotection pigments in stations 1 and 2 can be explained because of the lower incident UVR at the higher latitudes sampled and because induction of UVR defense mechanisms depends on the balance between irradiance and the energetic demands of phytoplankton metabolism (Smith and Cullen, 1995). Moreover, the waters of the HCS (mostly the southern stations) follows the optical characteristic of the coastal waters, which are characterized by a low penetration of UVR depending on the CDOM concentration (Tedetti and Sempéré, 2006). Häder et al. (2007) found a negative exponential relation between the depth that UVR penetrate and the concentration of CDOM and have highlighted that CDOM could be a mediator of climate- UV interactions. The high values of diffuse attenuation coefficients (Kd), for the southern stations, can be explained by high levels of DOM coming from an increase discharge of terrestrial soils due to the presence of rivers and a higher precipitation regime (Thatje *et al.*, 2008).

The proportion of the light that was absorbed by detrital particles was low, but increased at the stations corresponding to the lower latitudes sampled, that were more oligotrophic. This is in agreement with a large absorption by the detrital component in oligotrophic waters due to the higher presence of bacteria and detritus (Agustí and Cruzado, 1992). The higher penetration of UVR in the northern part of the HCS associated with high levels of irradiance can explain the absorption peaks in the range of 330-340 nm found in stations 3, 4 and 5 (figure 8), showing that these communities responds producing photoprotection pigments. Other consequence is the adjustment of depth at which the autotrophic community develops at most (DCM), which is deeper in the northern part than in the southern part (figure 9). This can be showing some avoidance reaction of phytoplankton to elevated levels of UVR (Reynolds, 2006).

In terms of global change, where the UVR is expected to be enhanced, response of the phytoplankton community in the northern part of the HCS should be a greater production of photoprotection pigments due to the fact that enhanced UVR resulted in a stimulation for Mycrosporine-like aminoacids (MAA's) (Smith and Cullen, 1995; Gabriela and Anne, 1998). For the southern part of these current systems this enhanced UVR can be a major threaten for the phytoplankton community, due for the lack of photoprotection pigments reported here. Montecino and Pizarro (1995) have pointed out that in presence of the effects of severe depletion of the ozone layer and enhanced levels of UVR, the phytoplankton community will be able to respond against this new threaten; but the ozone depletion isn't unique effect of global change and other important changes are predicted, like changes into the precipitation regimen (IPCC, 2007) which can affect the discharges of rivers and DOM of the waters and as a consequence change the water optics properties.

Finally, we can conclude that the HCS shows a clear pattern of higher penetration of UVR in the northern part than in the southern part, associated with the high irradiance levels and the constancy of clear skies in the northern part the autotrophic community respond with a production of photoprotection pigments, regulating their depth and modifying their autotrophic metabolism to a heterotrophic metabolism. In terms of Global Change, the diminishing of the ozone layer will lead important consequences for the plankton community in the HCS which might have consequences in the global balance of CO_2 into the atmosphere.

ACKNOWLEDGMENTS

I thank to International Laboratory of Global Change "LINCGlobal", for the enormous opportunity that was to participate into the campaign "Humboldt 2009" and especially to their directors, Dr. Juan Carlos Castilla and Dr. Carlos Duarte, because they gave to me a global vision of the human impacts over the global system. Thanks to Dra. Miriam Fernandez because she gave me the idea and the importance of develop a global master degree, and to Dra. Susana Agustí, for all her help with the sampling, analyses and writing of the manuscript. I would thank to the University of Illes Balears (UIB) for let us use their installations; otherwise this master can never be done. Thanks to Thanks to my family which is always supporting me and to my Master's partners that were, are and will be my friends.

REFERENCES

Agustí, S. and A. Cruzado. – 1992. Relationship between light absorption by pelagic particles and microplankton metabolic activity in the Gulf of Lions. . *Marine Ecology Progress Series*. 85: 283-287.

Andrés, M., C. Werlinger, M. Palacios, N.P. Navarro and P. Cuadra. – 2007. Effects of UVB radiation on the initial stages of growth of Gigartina skottsbergii, Sarcothalia crispata and Mazzaella laminarioides (Gigartinales, Rhodophyta), *Eighteenth International Seaweed Symposium,* pp. 225-233.

Atkinson, R.J. – 1997. Ozone variability over the southern hemisphere. *Australian Meteorological Magazine*. 46: 195-201.

Booth, C.R. and J.H. Morrow. – 1997. The Penetration of UV into Natural Waters. *Photochemistry and Photobiology*. 65: 254-257.

Bricaud, A. and D. Stramski. – 1990. Spectral Absorption-Coefficients of Living Phytoplankton and Nonalgal Biogenous Matter - a Comparison between the Peru Upwelling Area and the Sargasso Sea. *Limnology and Oceanography*. 35: 562-582.

Broitman, B.R., S.A. Navarrete, F. Smith and S.D. Gaines. – 2001. Geographic variation of southeastern Pacific intertidal communities. *Marine Ecology Progress Series*. 224: 21-34.

Cabrera, S., S. Bozzo and H. Fuenzalida. – 1995. Variations in UV radiation in Chile. *Journal of Photochemistry and Photobiology B: Biology*. 28: 137-142.

Crawley, M. – 2007. *The R Book*. Wiley Publishing, Imperial College London at Silwood Park, UK.

Duarte, C.M., J.C. Abanades, S. Agustí, S. Alonso, G. Benito, J.C. Ciscar, J. Dachs, J.O. Grimalt, I. López, C. Montes, M. Pardo, A.F. Ríos, R. Simó and F. Valladares. – 2009. *Cambio global. Impacto de la actividad humana sobre el sistema Tierra*. Consejo Superior de Investigaciones Científicas, CSIC y Los Libros de la Catarata., Madrid.

Dunlap, W.C. and J.M. Shick. – 1998. REVIEW—ULTRAVIOLET RADIATION-ABSORBING MYCOSPORINE-LIKE AMINO ACIDS IN CORAL REEF ORGANISMS: A BIOCHEMICAL AND ENVIRONMENTAL PERSPECTIVE. *Journal of Phycology*. 34: 418-430.

Fariña, J.M., M. Sepulveda, M.V. Reyna, K.P. Wallem and P.G. Ossa-Zazzali. – 2008. Geographical variation in the use of intertidal rocky shores by the lizard Microlophus atacamensis in relation to changes in terrestrial productivity along the Atacama Desert coast. *Journal of Animal Ecology*. 77: 458-468.

Fernández, M., A. Astorga, S.A. Navarrete, C. Valdovinos and P.A. Marquet. – 2009. Deconstructing latitudinal species richness patterns in the ocean: does larval development hold the clue? *Ecology Letters*. 12: 601-611.

Fernández, M. and A. Brante. – 2003. Brood care in Brachyuran crabs: the effect of oxygen provision on reproductive costs. *Revista chilena de historia natural*. 76: 157-168.

Fernández, M., E. Jaramillo, P.A. Marquet, C.A. Moreno, S.A. Navarrete, P.F. Ojeda, C.R. Valdovinos and J.A. Vásquez. – 2000. Diversity, dynamics and

biogeography of chilean benthic nearshore ecosystems: an overview and guidelines for conservation. *Revista Chilena de Historia Natural*. 73: 2-33.

Gabriela, H. and C.S. Anne. – 1998. Photoinduction of UV-absorbing compounds in six species of marine phytoplankton. *Marine Ecology Progress Series*. 174: 207-222.

Gebhardt, A., T. Petzoldt and M. Maechler. – 2009. Fortran code by H. Akima R port by Albrecht Gebhardt aspline function by Thomas Petzoldt <petzoldt@rcs.urz.tu-dresden.de> enhancements and corrections by Martin Maechler. Akima: Interpolation of irregularly spaced data. *R package version 0.5-4.* http://CRAN.R-project.org/package=akima.

Godoy, N., A. Canepa, S. Lasternas, E. Mayol, S. Agustí, J.C. Castilla and C.M. Duarte. – *in prep*. Impacts of UV radiation on plankton community metabolism along the Humboldt Current System.

Häder, D.-P., R.C. Worrest, H.D. Kumar and R.C. Smith. – 1995. Effects of Increased Solar Ultraviolet Radiation on Aquatic Ecosystems. *Ambio*. 24: 174-180.

Häder, D.P., H.D. Kumar, R.C. Smith and R.C. Worrest. – 1998. Effects on aquatic ecosystems. *Journal of Photochemistry and Photobiology B: Biology*. 46: 53-68.

Häder, D.P., H.D. Kumar, R.C. Smith and R.C. Worrest. – 2007. Effects of solar UV radiation on aquatic ecosystems and interactions with climate change. *Photochemical & Photobiological Sciences*. 6: 267-285.

Hardy, J. and H. Gucinski – 1989. Stratospheric ozone depletion: Implications for marine ecosystems. *Other Information: Pub. in Oceanography(Nov 1989).* PB-90-196601/XAB; EPA--600/J-89/301 United StatesTue Feb 12 16:04:25 EST 2008NTIS, PC A02/MF A01GRA; GRA-90-03169; EDB-90-095970; ERA-15-035783English: Medium: X; Size: Pages: (6 p).

Heberlein, C. and E. Bournay. – 2009. *Vital Ozone graphics 2.0. Climate Link*. UNEP, GRID-Arendal and Zoï Environment Network.

Helbling, W.E. and H. Zagarese. – 2003. *UV Effects in Aquatic Organisms and Ecosystems*. The Royal Society of Chemistry, Cambridge, UK.

IPCC. – 2007. Cambio Climático 2007: Informe de síntesis. Contribución de los Grupos de trabajo I, II y III al Cuarto informe de evaluación del Grupo Intergubernamental de Expertos sobre el Cambio Climático. In: R.K. Pachauri and A. Reisinger (eds.), pp. 104. IPCC, Ginebra, Suiza.

Jarah, A.M., J.B. Amy, C. Phillipe, H.J. Wade, J. Fabien, A.M. Joseph, J.D. Pakulski, S. Richard and L.M. David. – 2009. Sunlight-induced DNA Damage in Marine Micro-organisms Collected Along a Latitudinal Gradient from 70°N to 68°S. *Photochemistry and Photobiology*. 85: 412-420.

Latif, M. and N.S. Keenlyside. – 2008. El Niño/Southern Oscillation response to global warming. *Proceedings of the National Academy of Sciences*: -.

Lieselotte, R. and R. Dale. – 1997. Photoinduction of UV-absorbing compounds in Antarctic diatoms and Phaeocystis antarctica. *Marine Ecology Progress Series*. 160: 13-25.

Llabrés, M., S. Agustí, M. Fernández, A. Canepa, F. Maurin, F. Vidal and C.M. Duarte. – *Submitted*. Impact of Elevated UVB Radiation on Marine Biota. *Global Change Biology*. submitted.

Montecino, V. and G. Pizarro. – 1995. Phytoplankton acclimation and spectral penetration of UV irradiance off the central Chilean coast. *Marine Ecology Progress Series*. 121: 261-269.

Morales, C.E. and C.B. Lange. – 2004. Oceanographic studies in the Humboldt current system off Chile: an introduction. *Deep-Sea Research Part II*. 51: 2345-2348.

Morel, A., B. Gentili, H. Claustre, M. Babin, A. Bricaud, J. Ras and F. Tieche. – 2007. Optical properties of the "clearest" natural waters. *Limnology and Oceanography*. 52: 217-229.

Pelletier, É., P. Sargian, J. Payet and S. Demers. – 2006. Ecotoxicological Effects of Combined UVB and Organic Contaminants in Coastal Waters: A Review. *Photochemistry and Photobiology*. 82: 981-993.

Power, S.B. and I.N. Smith. – 2007. Weakening of the Walker Circulation and apparent dominance of El Niño both reach record levels, but has ENSO really changed? *Geophys. Res. Lett.*, 34.

Quinn, G.P. and M.J. Keough. – 2002. *Experimental Design and Data Analysis for Biologists*. Cambridge University Press, Cambridge, UK.

R Development Core Team. – 2010. R: A Language and Environment for Statistical Computing. *R Foundation for Statistical Computing, Viena, Austria. ISBN 3-900051-07-0. http://www.R-project.org.*

Ravishankara, A.R., J.S. Daniel and R.W. Portmann. – 2009. Nitrous Oxide (N2O): The Dominant Ozone-Depleting Substance Emitted in the 21st Century. *Science*. 326: 123-125.

Reynolds, C.S. – 2006. *The Ecology of Phytoplankton*. Cambridge University Press.

Singh, S.P., S. Kumari, R.P. Rastogi, K.L. Singh and R.P. Sinha. – 2008. Mycosporine-like amino acids (MAAs): chemical structure, biosynthesis and significance as UV-absorbing/screening compounds. *Indian Journal of Experimental Biology*. 46: 7-17.

Smith, R.C. and J.J. Cullen. – 1995. Effects of UV radiation on Phytoplankton. *Reviews of Geophysics*. SUPPLEMENT: 1211-1223.

Smith, R.C., B.B. Prezelin, K.S. Baker, R.R. Bidigare, N.P. Boucher, T. Coley, D. Karentz, S. MacIntyre, H.A. Matlick, D. Menzies, M. Ondrusek, Z. Wan and K.J. Waters. – 1992. Ozone Depletion: Ultraviolet Radiation and Phytoplankton Biology in Antarctic Waters. *Science*. 255: 952-959.

Solomon, S. – 1999. STRATOSPHERIC OZONE DEPLETION: A REVIEW OF CONCEPTS AND HISTORY. *Reviews of Geophysics*. 37: 275-316.

Tedetti, M. and R. Sempéré. – 2006. Penetration of Ultraviolet Radiation in the Marine Environment. A Review. *Photochemistry and Photobiology*. 82: 389-397.

Tedetti, M., R. Sempéré, A. Vasilkov, B. Charrière, D. Nérini, W.L. Miller, K. Kawamura and P. Raimbault. – 2007. High penetration of ultraviolet radiation in the south east Pacific waters. *Geophys. Res. Lett.*, 34.

Thatje, S., O. Heilmayer and J. Laudien. – 2008. Climate variability and El Niño Southern Oscillation: implications for natural coastal resources and management. *Helgoland Marine Research*. 62: S5-S14.

Thiel, M., E.C. Macaya, E. Acuña, W.E. Arntz, H. Bastias, K. Brokordt, P.A. Camus, J.C. Castilla, L.R. Castro, M. Cortés, C.P. Dumont, R. Escribano, M. Fernández, J.A. Gajardo, C.F. Gaymer, I. Gomez, A.E. González, H.E. González, P.A. Haye, J.-E. Illanes, J.L. Iriarte, D.A. Lancellotti, G. Luna-Jorquera, C. Luxoro, P.H. Manriquez, V. Marín, P. Muñoz, S.A. Navarrete, E. Perez, E. Poulin, J. Sellanes, H.H. Sepúlveda, W.B. Stotz, F. Tala, A. Thomas, C.A. Vargas, J.A. Vásquez and J.M. Alonso Vega. – 2007. The Humboldt Current System of Northen and Central Chile. Oceanographic Processes, Ecological Interactions

and Socioeconomic Feedback. *Oceanography and Marine Biology: An Annual Review*. 45: 195-344.

Varela, R.A., F.G. Figueiras, B. Arbones and S. Agustí. – 1998. Determining the Contribution of Pigments and the Nonalgal Fractions to Total Absorption: Toward an Improved Algorithm. *Limnology and Oceanography*. 43: 449-457.

Véliz, K., M. Edding, F. Tala and I. Gómez. – 2006. Effects of ultraviolet radiation on different life cycle stages of the south Pacific kelps, Lessonia nigrescens and Lessonia trabeculata (Laminariales, Phaeophyceae). *Marine Biology*. 149: 1015-1024.

Wahl, M., M. Molis, A. Davis, S. Dobretsov, S.T. Dürr, J. Johanssons, J. Kinley, D. Kirugara, M. Langer, H.K. Lotze, M. Thiel, J.C. Thomason, B. Worm and D. Zeevi Ben-Yosef. – 2004. UV effects that come and go: a global comparison of marine benthic community level impacts. *Global Change Biology*. 10: 1962-1972.

Weatherhead, E.C. and S.B. Andersen. – 2006. The search for signs of recovery of the ozone layer. *Nature*. 441: 39-45.

Whitehead, K. and M. Vernet. – 2000. Influence of mycosporine-like amino acids (MAAs) on UV absorption by particulate and dissolved organic matter in La Jolla Bay. *Limnology and Oceanography*. 45: 1788-1796.

Yaping, W., G. Kunshan, L. Gang and H. Eduardo Walter. – 2010. Seasonal Impacts of Solar UV Radiation on Photosynthesis of Phytoplankton Assemblages in the Coastal Waters of the South China Sea. *Photochemistry and Photobiology*. 86: 586-592.